Australian Earthquake Engineering Society 2010 Conference, Perth, Western Australia

Pounding response of adjacent bridge structures on a canyon site to spatially varying ground motions

Kaiming Bi[1], Hong Hao[2]

[1]PhD student, School of Civil and Resource Engineering, The University of Western Australia, WA. Email: bkm@civil.uwa.edu.au
[2]Professor, School of Civil and Resource Engineering, The University of Western Australia, WA. Email: hao@civil.uwa.edu.au

Abstract

Poundings between adjacent bridge structures were observed in almost all the major earthquakes in the past. Previous studies of pounding responses of adjacent bridge structures were usually based on the simplified lumped mass model or beam-column element model. Therefore, only point to point pounding in 1D, usually the axial direction of the structures, was considered. In a real bridge structure under seismic loading, pounding could be between the entire surfaces of the adjacent decks, torsional responses of the adjacent decks may induce eccentric poundings at corners besides those at the geometric centre of the adjacent deck cross sections. The surface to surface, and eccentric poundings were usually not considered in previous studies. To more realistically study the pounding responses, a 3D finite element model of a two-span simply-supported bridge located on a canyon site is established in the present study. The spatially varying ground motions in the three directions at foundations of the bridge structures are simulated based on the combined spectral representation method and one dimensional wave propagation theory. The pounding effects of the adjacent bridge structures under multi-component spatially varying ground motions are investigated by using the finite element code LS-DYNA. Numerical results show that detailed 3D finite element model is necessary for a comprehensive analysis of pounding between adjacent bridge structures because surface to surface pounding and torsional response induced eccentric pounding, which can not be modelled in the commonly adopted 1D model, result in very different pounding responses as compared to the point to point poundings assumed occurring at the geometric centre of the adjacent bridge decks.

Keywords: pounding effect, 3D FEM, torsional responses, multi-component spatially varying ground motions

1. Introduction

Damage of adjacent bridge structures due to out-of-phase responses such as pounding and unseating have been observed in almost all the major earthquakes. Pounding is an extremely complex phenomenon involving damage due to plastic deformation at contact points, local cracking or crushing, fracturing due to impact, friction, etc. To simplify the analysis, most previous studies of pounding responses of adjacent bridge structures were usually based on the simplified lumped mass model [1-6] or beam-column element model [7, 8]. Therefore, only point to point pounding in 1D, usually

the axial direction of the structures, was considered. In a real bridge structure under seismic loading, pounding could be between the entire surfaces of the adjacent structures, torsional responses may also induce additional poundings at corners of the adjacent decks besides those at the geometric centre of the deck cross sections. To more realistically study the pounding phenomenon between adjacent bridge structures, a detailed 3D finite element analysis is necessary. Zanardo et al. [9] modelled the box-section bridge girders with shell elements and piers with beam-column elements, and carried out a parametrical study of pounding phenomenon of a multi-span simply-supported bridge with base isolation devices. Julian et al. [10] evaluated the effectiveness of cable restrainers to mitigate earthquake damage through connection between isolated and non-isolated sections of curved steel viaducts using three-dimensional non-linear finite element response analysis. Although 3D FE model of bridge structures were developed in those two studies [9,10], the surface to surface pounding were not considered. The pounding phenomenon in these studies was simulated by the contact elements which linked the external nodes of adjacent segments together. Zhu et al. [11] proposed a 3D contact-friction model to analyse pounding between bridge girders. They also analysed the effectiveness of different countermeasures to mitigate detrimental pounding between girders of a three-span steel bridge [12]. This latter method, however, could not model material non-linearities during contacts, and the task to search contact pairs is very time consuming and the searching algorithm is relatively complicated. More recently, Jankowski [13] analyzed the earthquake-induced pounding between the main building and the stairway tower of the Olive View Hospital based on the non-linear finite element method (FEM), and concluded that the use of FEM with a detailed representation of the geometry and the non-linear material behaviour makes the study of the earthquake-induced poundings more reliable than using discrete lumped mass or beam-column element models. To the best knowledge of the authors, the study of surface to surface, and torsional response induced eccentric pounding between adjacent bridge structures based on a detailed 3D FEM has not been reported yet.

In the present study, the pounding response between the abutment and the bridge deck and between two adjacent bridge decks of a two-span simply-supported bridge located on a canyon site is investigated. The detailed 3D finite element model of the bridge is constructed by using finite element code ANSYS [14]. LS-DYNA [15] is then employed to calculate the structural responses. The three-directional spatially varying ground motions at different foundations of the bridge are simulated based on the combined spectral representation method and one dimensional wave propagation theory [16]. The influence of pounding effect is investigated in detail. It should be noted that the material non-linearities and pounding induced local damage are not considered in the present study, which will be included in the subsequent studies.

2. Bridge and ground motion model

Figure 1(a) shows the elevation view of a two-span simply-supported bridge crossing a canyon site. The box-section bridge girders with the cross section shown in Figure 1(b) have the same span length of 50m. The Young's modulus and density of the bridge girders are 3.45×10^{10} Pa and 2500 kg/m^3, respectively. The L-type abutment is 8.1m long in transverse direction and its cross section is shown in Figure 1(c). The height of the rectangular central pier is 20m, with the cross section shown in Figure 1(d). The materials for the two abutments and the pier are the same, with Young's modulus and density of 3.0×10^{10} Pa and 2400 kg/m^3, respectively. The two bridge

girders are supported by 8 high-damping rubber bearings. The horizontal effective stiffness and equivalent damping ratio of a bearing are 2.33×10^7 N/m and 0.14 respectively [2, 9]. The stiffness of the bearing in the vertical direction is much larger than those in the horizontal directions, and is assumed to be 1.87×10^{10} N/m [9]. To allow for contraction and expansion of the bridge decks from creep, shrinkage, temperature fluctuations and traffic without generating constraint forces in the structure, a 5cm expansion joint is introduced between the abutments and the bridge decks and between the adjacent bridge decks. It is noted that the lateral side stoppers, which are usually installed in real engineering practice, are not considered in the model. The bridge girders can vibrate freely in the lateral direction (z direction) when poundings are not involved.

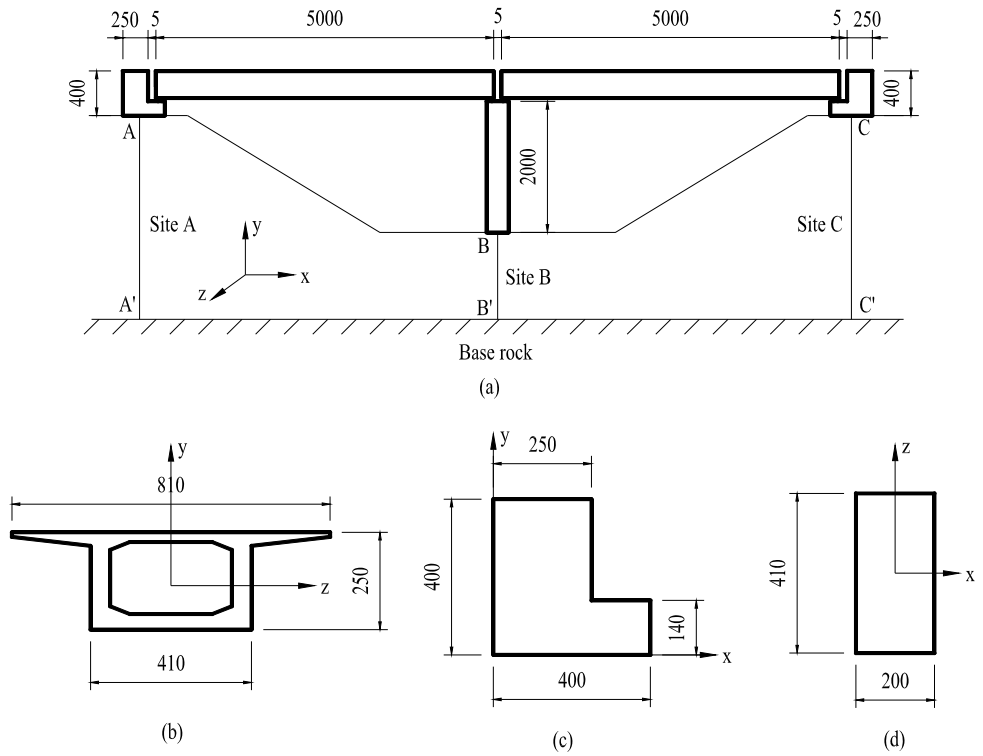

Figure 1. (a) Elevation view of the bridge, (b) Cross-section of the bridge girder, (c) Cross-section of the abutment and (d) Cross-section of the pier (unit: cm).

The bridge locates on a canyon site, consisting of horizontally extended soil layers on a half-space (base rock). The foundations of the bridge are assumed rigidly fixed to the ground surface and soil-structure interaction (SSI) is not involved. Points A, B and C are the three bridge support locations on the ground surface, the corresponding points on the base rock are A', B' and C'.

The 3D finite element model of the bridge is constructed by using the finite element code ANSYS [14]. The bridge girders, abutments and pier are modelled by eight-node solid elements. The bearings are modelled by the spring-dashpot elements. The detailed geometric characteristics in Figure 1 and the material properties have been implemented in the model. 85428 nodes and 59824 elements are included in the finite element model. Figure 2 shows the first four vibration frequencies and the corresponding mode shapes of the bridge. As shown, the first four vibration frequencies of the bridge are 1.018, 1.138, 1.254 and 1.313Hz for the in-phase

longitudinal (x direction), in-phase transverse (z direction), out-of-phase transverse and out-of-phase longitudinal vibrations, respectively.

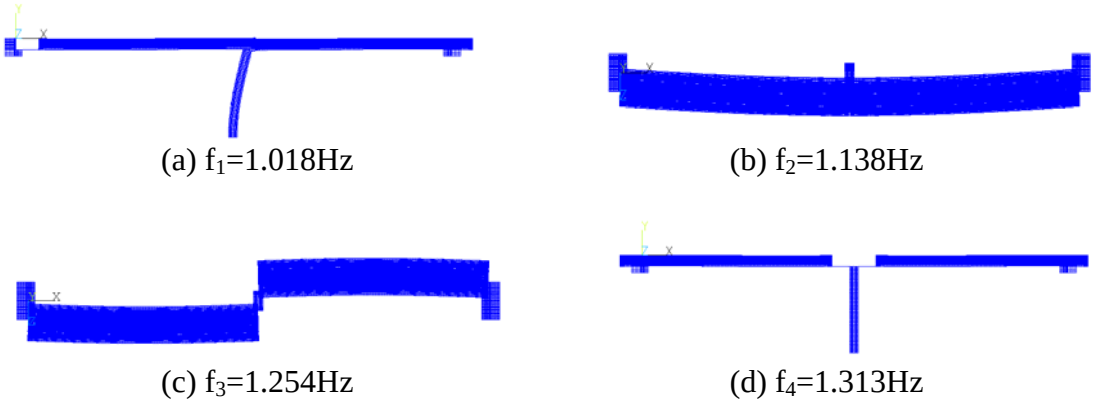

(a) f_1=1.018Hz (b) f_2=1.138Hz

(c) f_3=1.254Hz (d) f_4=1.313Hz

Figure 2. First four vibration frequencies and modes of the bridge

Rayleigh damping is assumed in the model to simulate energy dissipation during structural vibrations. By assuming a structural damping ratio of 5%, and with the first two vibration frequencies in Figure 2, the mass matrix multiplier is 0.3376 and the stiffness matrix multiplier is 0.0074 in the present study.

Poundings may occur between the abutment and the bridge girder and/or between two adjacent bridge girders. The treatment of sliding and impact along interfaces of different elements is an important issue in finite element modelling. To realistically consider the poundings between entire surfaces of adjacent structures, the contact type of *CONTACT_AUTOMATIC_SURFACE_TO_SURFACE in LS-DYNA [15] is employed in the simulations. The Coulomb friction coefficient of 0.5 is assumed in the analysis [13].

In the present study, only one soil layer is considered and soil conditions for the three sites are assumed to be the same with the corresponding parameters for the base rock and soil shown in Table I. Soil depths for the three sites are 48.6, 30 and 48.6m respectively. The horizontal in-plane, horizontal out-of-plane and vertical in-plane spatially varying ground motions at different supports of the bridge are stochastically simulated based on the combined spectral representation method and one dimensional wave propagation theory [16], and are applied simultaneously to the longitudinal, transverse and vertical directions of the bridge. Figure 3 shows the spatially varying displacements at different supports in the three directions.

Table I. Parameters for local site conditions.

Type	Density (kg/m^3)	Shear modulus(MPa)	Damping ratio	Poisson's ratio
Base rock	2500	1800	0.05	0.33
Soil	2000	320	0.05	0.4

3. Numerical results

The earthquake-induced responses of the two-span simply-supported bridge shown in Figure 1 are investigated in this section. The time step of $\Delta t = 0.002\,\mathrm{s}$ is used in the present study. This time step guarantees numerical stability and accuracy based on the

preliminary simulations, which are not shown here for page limitation. For comparison purpose, the case without pounding is also considered, which is achieved by assuming the separation gaps between the abutments and the girders and between two adjacent girders are large enough so that pounding phenomenon can be completely precluded and the structure vibrates freely. To obtain a less biased estimation, 3 sets of spatially varying ground motions are used, the results presented here are the assembled-mean responses.

Poundings may occur between the abutments and bridge girders and between two bridge girders as mentioned above. Though the bridge considered in the present paper is a symmetrical structure, the responses of different parts will be different owing to ground motion spatial variations and pounding effects. To obtain a general idea of the earthquake-induced structural responses, the following 12 nodes as shown in Figure 4 are selected to examine the results. The peak responses, which are mostly concerned in engineering practice, are listed in Table II, where the torsional responses is illustrated by the relative longitudinal displacements between the inside node and corresponding outside node at the same section.

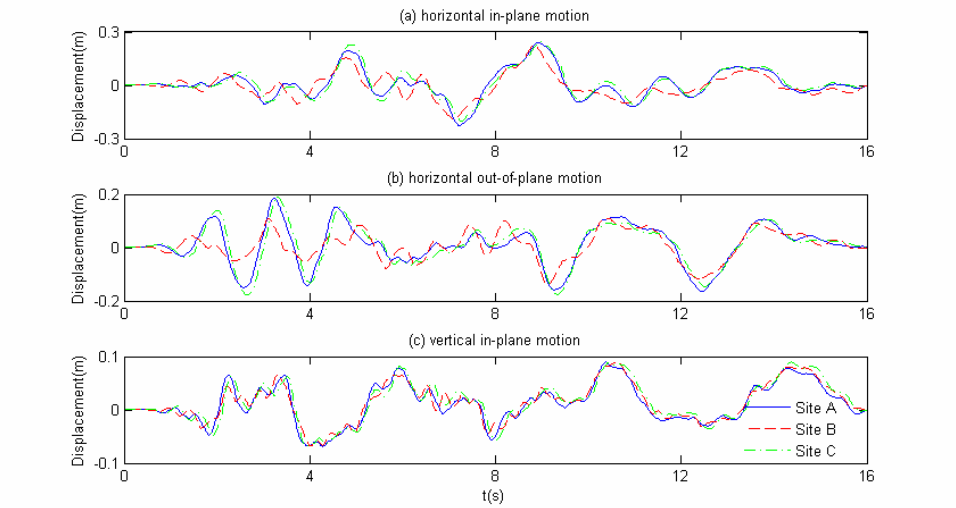

Figure 3. Spatially varying displacements.

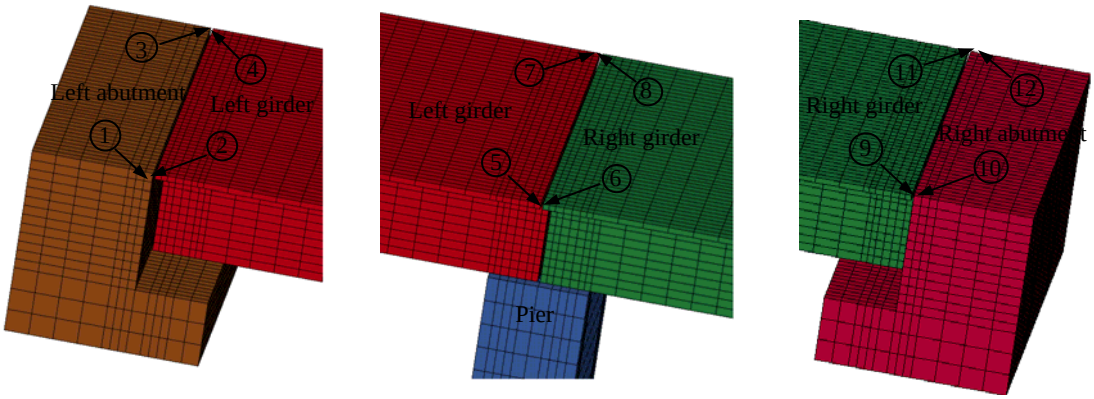

Figure 4. Different nodes examined in the present study.

It can be noted in Table II that the responses of the abutments are almost unaffected by pounding. This is because the abutment is quite rigid compared to the adjacent girder. Similar observations were obtained by Maragakis et al. [17], who investigated the influences of abutment and deck stiffness, gap, and deck to abutment mass ratio

on the pounding responses between abutments and bridge decks, and concluded that pounding effect on rigid abutment is not evident. The influence of collisions on the girder response is, however, significant. Poundings usually result in smaller displacements in the longitudinal direction. This is because the rigid abutment acts as a constraint to the flexible girder. For the displacements in the transverse and vertical directions, smaller values are also observed when poundings are involved. This may be because of the friction forces between the adjacent surfaces during poundings, which reduces the displacement responses of the bridge structures in the transverse and vertical directions. Pounding effects, however, result in larger torsional responses as shown in the last two columns of Table II. This is because spatially varying ground motions cause torsional responses of the deck, which results in unsymmetrical pounding forces over the deck surface. The eccentric pounding in turn further intensifies the torsional responses.

Table II. Influence of pounding effect on the mean peak displacements (m).

Node	Longitudinal		Transverse		Vertical		Torsional	
	with	Without	with	without	with	without	with	Without
1	0.181	0.182	0.135	0.135	0.072	0.072	0.0045	0.0002
3	0.182	0.182	0.135	0.135	0.072	0.072		
2	0.210	0.274	0.184	0.207	0.098	0.186	0.0418	0.0373
4	0.217	0.287	0.184	0.206	0.102	0.161		
5	0.208	0.266	0.270	0.263	0.100	0.201	0.0354	0.0304
7	0.209	0.275	0.269	0.262	0.104	0.129		
6	0.233	0.272	0.241	0.293	0.136	0.133	0.0371	0.0321
8	0.237	0.261	0.240	0.292	0.138	0.143		
9	0.226	0.267	0.179	0.200	0.096	0.109	0.0454	0.0371
11	0.220	0.255	0.178	0.197	0.112	0.107		
10	0.179	0.179	0.119	0.119	0.067	0.067	0.0024	0.0001
12	0.179	0.179	0.119	0.119	0.067	0.067		

It also can be seen from the table that the maximum torisonal response can be as large as the gap size, i.e. 5cm in the present study, implying the occurrence of torsional response induced eccentric poundings at the corner points of the bridge deck indicated in Figure 4. To examine the occurrence of poundings, the longitudinal displacements of nodes 1 and 2 and node 3 and 4 are plotted in the same figure with the displacements of nodes 1 and 3 shifted by the initial gap of 5cm. Thus, in these figures, the instants where the displacements of the two adjacent points coinciding with each other indicate the occurrence of poundings. As shown in Figure 5(a), node 1 and node 2 come into contacts 15 times, at the time instant at 3.26, 5.29, 6.29, 6.68, 7.30, 7.72, 8.20, 8.63, 9.13, 9.66, 11.13, 11.89, 12.44, 13.70 and 14.26s. Whereas for nodes 3 and 4, the poundings at 6.29, 11.89 and 12.44s do not occur, but two more collides can be observed at 3.76 and 13.20s. Since these points locate at the opposite corners of the bridge deck cross section, pounding at these points occurring simultaneously implies the entire cross sections are in contact, i.e., surface to surface pounding occurs. Otherwise, they are torsional response induced eccentric poundings. In this example, pounding occurring at 6.29s, 11.89s and 12.44s are eccentric pounding between nodes 1 and 2, and those at 3.76s and 13.20s are eccentric pounding between nodes 3 and 4. Torsional response induced eccentric pounding between other corner points shown in Figure 4 are also observed. Owing to page limit, they are not shown here.

By using the traditional lumped-mass model or beam-column element model, the differences of the stress on the entire contact surface can not be obtained. However, the use of 3D finite element model allows a more detailed prediction of the largest stresses and its locations, where earthquake-induced damage may occur. Figure 6 shows the stress distributions in the longitudinal direction at the left abutment with and without pounding effect at t=6.27s. This time instant is selected because the resultant pounding force reaches the maximum value. As shown in Figure 6(a), the maximum longitudinal stress at the bottom outside corner of the bridge girder reaches around 90MPa. This value is much larger than the compressive strength of concrete, which is usually 30-65MPa for impact loading [18], thus concrete damage are expected. These results are consistent with the observations in the past major earthquakes, in which the damage around the corners of the structure were usually the most serious. Compared with Figure 6(b), it is obvious that pounding effect significantly increases the intensity of longitudinal stresses.

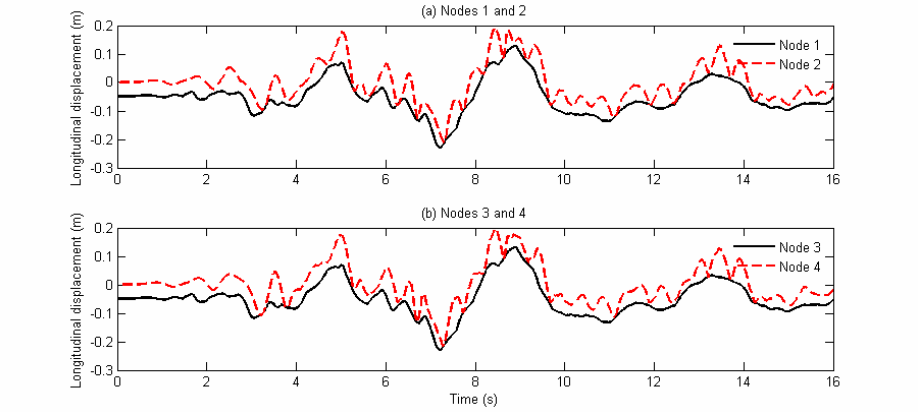

Figure 5. Longitudinal displacements of different nodes with pounding effects (a) nodes 1 and 2 and (b) nodes 3 and 4.

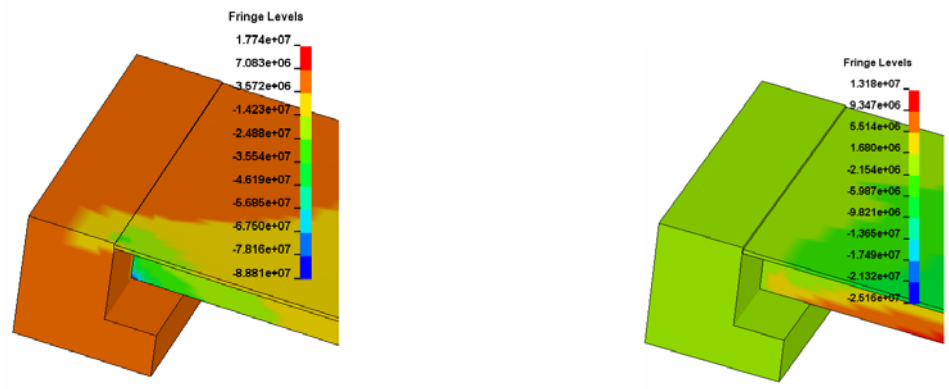

(a) (b)

Figure 6. Stresses in the longitudinal direction at left abutment when t=6.27s (a) with pounding and (b) without pounding (unit: Pa)

4. Conclusions

Based on a detailed 3D finite element model, the earthquake-induced pounding responses between adjacent components of a two-span simply-supported bridge structure located at a canyon site are studied in the present paper. It is found that a

detailed 3D finite element model gives more detailed predictions of the earthquake-induced pounding responses of bridge structures since torsional vibrations of the structure, which play an important role in the overall structure response, can be modelled. With a 3D model, the potential damage locations in the structure can be identified. Pounding effects usually results in smaller longitudinal, transverse and vertical displacements while lead to larger torsional responses.

References

1. Malhotra PK. Dynamics of seismic pounding at expansion joints of concrete `bridges. *Journal of Engineering Mechanics* 1998; **124**(7):794-802.
2. Jankowski R, Wilde K, Fujino Y. Pounding of superstructure segments in isolated elevated bridge during earthquakes. *Earthquake Engineering and Structural Dynamics* 1998; **27**:487-502.
3. Ruangrassamee A, Kawashima K. Relative displacement response spectra with pounding effect. *Earthquake Engineering and Structural Dynamics* 2001; **30**(10): 1511-1538.
4. DesRoches R, Muthukumar S. Effect of pounding and restrainers on seismic response of multi-frame bridges. *Journal of Structural Engineering* (ASCE) 2002; **128**(7): 860-869.
5. Chouw N, Hao H. Study of SSI and non-uniform ground motion effects on pounding between bridge girders. *Soil Dynamics and Earthquake Engineering* 2005; **23**:717-728.
6. Chouw N, Hao H. Significance of SSI and non-uniform near-fault ground motions in bridge response I: Effect on response with conventional expansion joint. *Engineering Structures* 2008; **30**(1):141-153.
7. Jankowski R, Wilde K, Fujino Y. Reduction of pounding effects in elevated bridges during earthquakes. *Earthquake Engineering and Structural Dynamics* 2000; **29**: 195-212.
8. Chouw N, Hao H, Su H. Multi-sided pounding response of bridge structures with non-linear bearings to spatially varying ground excitation. *Advances in Structural Engineering* 2006; **9**(1):55-66.
9. Zanardo G, Hao H, Modena C. Seismic response of multi-span simply supported bridges to spatially varying earthquake ground motion. *Earthquake Engineering and Structural Dynamics* 2002; **31**(6): 1325-1345.
10. Julian FDR, Hayashikawa T, Obata T. Seismic performance of isolated curved steel viaducts equipped with deck unseating prevention cable restrainers. *Journal of Constructional Steel Research* 2006; **63**:237-253.
11. Zhu P, Abe M, Fujino Y. Modelling three-dimensional non-linear seismic performance of elevated bridges with emphasis on pounding of girders. *Earthquake Engineering and Structural Dynamics* 2002; **31**:1891-1913.
12. Zhu P, Abe M, Fujino Y. Evaluation of pounding countermeasures and serviceability of elevated bridges during seismic excitation using 3D modelling. *Earthquake Engineering and Structural Dynamics* 2004; **33**:591-609.
13. Jankowski R. Non-linear FEM analysis of earthquake-induced pounding between the main building and the stairway tower of the Olive View Hospital. *Engineering Structures* 2009; **31**:1851-1864.
14. ANSYS. *ANSYS user's manual revision 12.1*. ANSYS Inc, USA, 2009.
15. LS-DYNA. *LS-DYNA user manual*. Livermore Software Technology Corporation: California, USA, 2007.
16. Bi K, Hao H. Influence of irregular topography and random soil properties on coherency loss of spatial seismic ground motions. *Earthquake Engineering and Structural Dynamics* 2010 (in print).
17. Maragakis E, Douglas B, Vrontinos S. Classical formulations of the impact between bridge deck and abutments during strong earthquake. Proceedings of the 6th Canadian Conference on Earthquake Engineering, Toronto, Canada, 1991; 205-212
18. Bischoff PH, Perry SH. Impact behaviour of plain concrete loaded in uniaxial compression. *Journal of Engineering Mechanics* 1995; **121**(6): 685-693.